Available online at www.sciencedirect.com
ScienceDirect
Carbohydrate Polymers 72 (2008) 122–127
Carbohydrate Polymers
www.elsevier.com/locate/carbpol

Arrangement of cellulose microfibrils in the wheat straw cell wall

Hui Yu [a,b], Ruigang Liu [a,*], Dawa Shen [a], Zhonghua Wu [c], Yong Huang [a,d,*]

[a] State Key Laboratory of Polymer Physics and Chemistry, Joint Laboratory of Polymer Science and Material, Beijing National Laboratory for Molecular Sciences, Institute of Chemistry, CAS, Beijing 100080, China
[b] Graduate University, Chinese Academy of Sciences, Beijing 100039, China
[c] Institute of High Energy Physics, Chinese Academy of Sciences, Beijing 100049, China
[d] Laboratory of Cellulose and Lignocellulosics Chemistry, Guangzhou Institute of Chemistry, Chinese Academy of Sciences, Guangzhou 510650, China

Received 21 January 2007; received in revised form 23 July 2007; accepted 25 July 2007
Available online 3 August 2007

Abstract

The arrangement of cellulose microfibrils in the cell wall from different tissues of wheat straw was investigated mainly using atomic force microscope (AFM). It was revealed that cellulose microfibrillar crystals arrange randomly in the parenchyma cell walls and are ordered quite well longitudinal to the fiber axis in the epidermal fibers. The microfibrillar crystals are about 20 nm in diameter and 150–200 nm in length. Moreover, the cellulose microfibrillar crystals in the epidermal fibers align periodically along the fiber axis and the periodicity is similar to the length of the fibrillar crystals. This structure was confirmed by small angle X-ray scattering (SAXS).

Keywords: Cellulose; Microfibrils; Morphology; Atomic force microscope (AFM)

1. Introduction

Wheat straw is one of the abundant renewable cellulose resources and has potential utilization in many fields. The cellulose fibers represent the valuable raw material for the paper industry and building board, and the microfibrils in composites (Dufresne, Kellerhals, & Witholt, 1999; Gousse, Chanzy, Cerrada, & Fleury, 2004; Helbert, Cavaille, & Dufresne, 1996; Liu, Mohanty, Askeland, Drzal, & Misra, 2004; Puglia, Tomassucci, & Kenny, 2003; Samir, Alloin, Sanchez, & Dufresne, 2004). In addition, some useful chemical compounds such as ethanol can be prepared from wheat straw (Demirbas, 2004; Kondoh, Oginuma, Umeda, & Umeda, 2005).

Wheat straw is mainly composed of cell walls in which cellulose is one of the main components. In the cell walls, the parallel cellulose chains bind together by hydrogen bonds to form microfibrils with several nanometers in diameter and millimeters in length. These high tensile strength crystalline microfibrils are the fundamental structure unit in plant cell walls. They make the major contribution to the mechanical strength of the plant cell walls and act as the framework thereof. The microfibrils are bonded by a gel matrix composed of hemicelluloses, lignin and other carbohydrate polymers to form a bio-composite (Campbell, 1993; Carpita & Gibeaut, 1993; Hanley, Revol, Godbout, & Gray, 1997; Thimm, Burritt, Ducker, & Melton, 2000). It is known that the arrangement and orientation of cellulose microfibrils in the cell wall are very important because it determines the capacity and direction of deformation of the cell wall (Taiz & Zeiger, 1991). The chemical structure of cellulose is well known. However, many questions on the details of the superstructure of native cellulose still remain open. More recently, many efforts have been made on the studies of the superstructure of native cellulose by atomic force microscopy (AFM)

* Corresponding authors. Address: State Key Laboratory of Polymer Physics and Chemistry, Joint Laboratory of Polymer Science and Material, Beijing National Laboratory for Molecular Sciences, Institute of Chemistry, CAS, Beijing 100080, China. Tel.: +86 10 82618573; fax: +86 10 62559373.
E-mail addresses: rgliu@iccas.ac.cn (R. Liu), yhuang@cashq.ac.cn (Y. Huang).

0144-8617/$ - see front matter © 2007 Elsevier Ltd. All rights reserved.
doi:10.1016/j.carbpol.2007.07.035

(Baker, Helbert, Sugiyama, & Miles, 1998; Davies & Harris, 2003; Gunning et al., 1998; Gustafsson, Ciovica, & Peltonen, 2003; Hanley et al., 1997; Pesacreta, Carlson, & Triplett, 1997; Simola, Malkavaara, Alen, & Peltonen, 2000; Thimm et al., 2000; Yan, Li, Yang, & Zhu, 2004) and transmission electron microscopy (TEM) (Hanley, Giasson, Revol, & Gray, 1992; Hanley et al., 1997; Kim, Imai, Wada, & Sugiyama, 2006). In our previous work, we had studied the orientation and morphology of cellulose in some special part, such as ring and spiral structure (Liu, Yu, & Huang, 2005; Yu, Liu, Shen, Jiang, & Huang, 2005). Even the experimental data growing in literature, there are still many unclear problems of native cellulose, such as the super-molecular structure, due to its variation in origins of cell types and plants. The structure of cell walls, which is selected by nature and has the optimism structure, properties and function relationship, is a perfect example of composites. To understand the compositions, composition distribution as well as inter-surface between different compositions can absolutely shed some light on preparing man-made composites.

In this paper, the arrangement and the morphology of the cellulose microfibrils in the cell wall from parenchyma cell wall and epidermal fibers of wheat straw were revealed by atomic force microscope (AFM), polarized optical microscope (POM), scanning electron microscope (SEM) and synchrotron radiation small angle X-ray scattering (SAXS).

2. Experimental

Mature wheat straw was collected from the experimental field of the Agriculture University of China. After being cleaned and dried, the wheat straw was cut into small pieces with about 1 cm in length. The small pieces of wheat straw were then disencrusted thoroughly with a purification method (Liu et al., 2005; Yu et al., 2005) to remove pectin, polysaccharides, lignin and other non-cellulosic substances completely.

The cellulose isolated from wheat straw was dispersed in distilled water by ultrasonic. The suspension of cellulose was then dropped onto a clean glass slide and air-dried. These samples were used for POM, AFM and SEM experiments. The samples used for SAXS were the mature raw wheat straw without extraction treatment. Sections with a thickness of 0.2 mm were cut carefully from the inner layer of the straw along the filament direction and only the epidermal layer was left, following which the epidermal layer of the straw was washed thoroughly with distilled water and then air-dried.

POM experiments were performed on an Olympus microscopy (BH-2) under crossing polarized light.

SEM measurements were carried out on a Hitachi S-4300 SEM, operated at 10 kV acceleration voltage. The sample was coated with platinum by an ion sputter.

AFM images were obtained on a NanoScope III Multi-Mode atomic force microscopy (Digital Instruments). Silicon cantilever tip with a resonance frequency of approximately 300 kHz and with a spring constant of about 32 N m^{-1} was used. The scan rate varied from 0.5 to 1.5 Hz. The typical value for the amplitude was 2.0 V, and the set point amplitude ratio ($r_{sp} = A_{sp}/A_0$, where A_{sp} is the set-point amplitude and A_0 is the amplitude of the free oscillation) was adjusted to 0.7–0.9. The integral gain, proportional gain and set-point were chosen so that the surface was tracked while maintaining the necessary contact with the sample. All images were measured at 512×512 pixel at ambient condition.

SAXS experiments were performed at beam line 4B9A of Beijing Synchrotron Radiation Facility (BSRF). The wavelength of the X-ray was 1.54 Å. The two-dimensional scattering data obtained were circularly averaged to transform one-dimensional scattering data and analyzed by subtracting the background noise.

3. Results and discussion

Macroscopically, a wheat straw stem is formed as concentric rings leaving a lumen in the center (Fig. 1). The outermost side of the stem is the dense epidermis layer (position a in Fig. 1), which gives additional mechanical strength to the stem and inhibits evaporation, beneath which is a loose layer containing parenchyma and vascular bundles (position b and d, respectively, in Fig. 1) (Hornsby, Hinrichsen, & Tarverdi, 1997). The parenchyma cell is important for plant "work", such as the photosynthesis and carbohydrate storage occurs in the parenchyma cells, and the water and solutes transport throughout the plant.

Fig. 2 shows the POM micrograph of the parenchyma cell walls and its typical AFM phase image. The parenchyma cells of wheat straw are typically around 100 μm

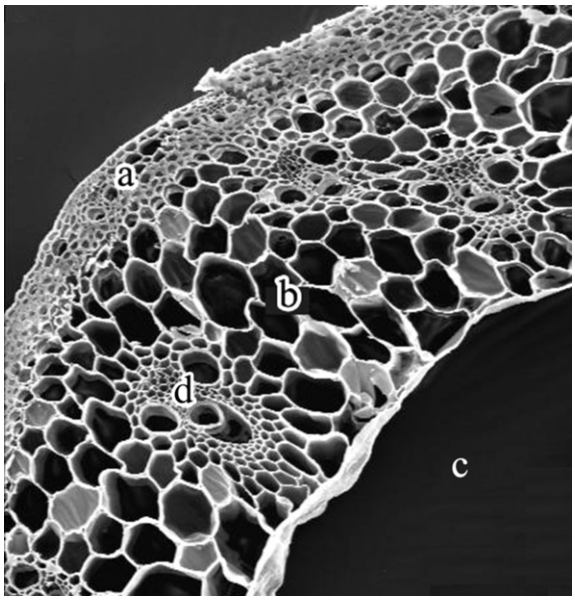

Fig. 1. Cross section of wheat straw. (a) epidermis, (b) parenchyma, (c) lumen and (d) vascular bundles.

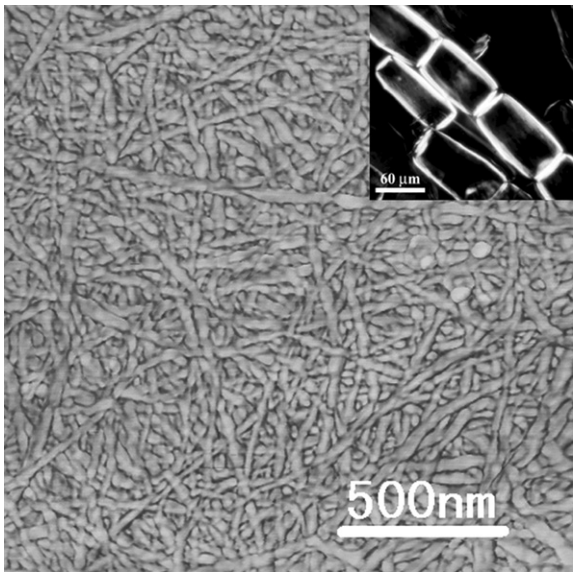

Fig. 2. Cellulose microfibrils arrangement in the parenchyma cell wall of wheat straw. AFM phase image. Inset: POM micrograph.

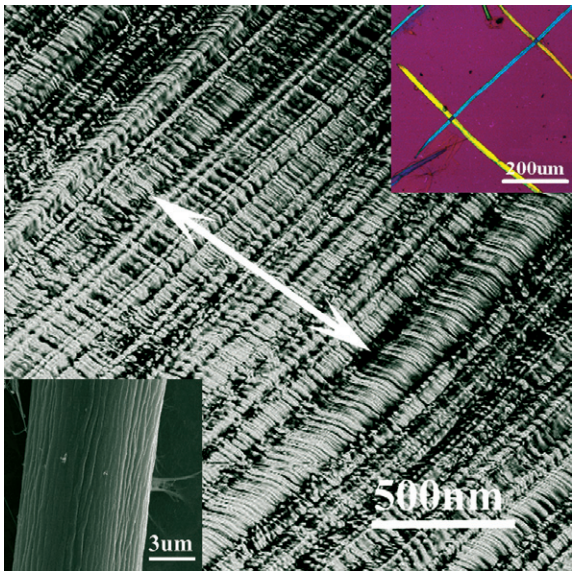

Fig. 3. Arrangement of cellulose microfibrils in epidermal fiber of wheat straw. AFM phase image. Inset images are POM micrograph λ-plate and SEM micrograph of the epidermal fiber, up right corner and lower left corner, respectively.

in length and about 60 μm in width (inset figure). Weak birefringence observed under POM indicates that there are cellulose crystals in the cell wall. However, no preferred orientation was observed by using cross polarized light with a first-order retardation plate (λ-plate), which is further confirmed by AFM phase image as shown in Fig. 2. The AFM phase image clearly shows the morphology of the cellulose microfibrils in the parenchyma cell walls of wheat straw. It is indicated that the cellulose microfibrils in the parenchyma cell walls have an interwoven network texture, in which the cellulose microfibrils interweave tightly and randomly like a non-woven fabric without any preferred orientation. The cellulose microfibrils are typically 20–30 nm in diameter and 100 nm to several micrometers in length. This arrangement of cellulose microfibrils is helpful to keep the parenchyma cell in shape and strengthens the cell walls. The cellulose microfibrils in the parenchyma cell walls of wheat straw are less uniform in diameter and less in aligning order than those in the primary cell walls of apple, Chinese water chestnut, potato, carrot (Baker et al., 1998), parenchyma cell walls of Celery (*Apium graveolens* L.) (Thimm et al., 2000), and primary cell walls of onion (Maximova, Osterberg, Koljonen, & Stenius, 2001).

The epidermis part of wheat straw has a much more dense structure than that of parenchyma as shown in Fig. 1. This part plays a key role for supporting the wheat straw to stand the outer forces such as wind. In our earlier work (Liu et al., 2005), the SEM results indicated that the epidermal cellulose fibers are well aligned along the longitude of wheat straw stem, which was confirmed by FTIR. Here in this work, the AFM observations provide more details of the cellulose microfibrils in the epidermal cellulose fibers. Fig. 3 shows the results of POM, SEM and AFM of the epidermal cellulose fibers. POM results show strong birefringence of the cellulose fibers (Fig. 3, top-right inset micrograph). With the application of a first-order retardation plate (λ-plate) under cross polarized light with, the epidermal fibers are blue in the first and third quadrants and yellow in the second and fourth quadrants. The results indicate a positive optical property of the epidermal cellulose fiber and suggest that cellulose chains orient in the longitudinal direction of fibers. The images of the scanning electron microscope (SEM) reveal the topography of a whole epidermal fiber. SEM micrograph (Fig. 3, low-left inset micrograph) indicates fibrillar structure that well aligns fiber longitudinal direction. The orientation of the fibrillar structure in the epidermal fiber of wheat straw can be further confirmed by AFM as shown in Fig. 3, in which the double-head arrows indicates the longitudinal axis of the fiber. The AFM results are in agreement with that of FTIR (Liu et al., 2005). Furthermore, the cellulose microfibrillar crystals in the epidermal fiber of wheat straw show almost uniform diameter of around 20 nm, which is similar to those of Valonia (Hanley et al., 1992). In the cellulose microfibrils of this dimension, there could be more than 1000 cellulose chains all aligned parallel in a related perfect crystalline array. In general, cellulose chains are parallel to each other in the cellulose crystal unit and are arranged along the longitudinal direction of the microfibrillar crystals (Chanzy & Henrissat, 1985; Koyama, Helbert, Imai, Sugiyama, & Henrissat, 1997). Meanwhile, there is no apparent lateral association or interwoven between the microfibrils.

The more interesting is that the microfibrillar crystals align orderly along the fiber axis with a periodicity of around 150–200 nm, which is shown clearly in the AFM phase image (Fig. 3). In order to understand the structure in more details, the epidermal fibers of wheat straw were

hydrolyzed in a 2.5 M HCl aqueous solution, in which the cellulose microfibrils were normally hydrolyzed in the amorphous regions at the end tips of the cellulose fibrillar crystals. AFM image of cellulose micro-crystals after hydrolyzation is shown in Fig. 4 and it can be found that the diameter of the cellulose micro-crystals is about 20 nm and the length is about 150–200 nm. It is suggested that microfibrillar crystals in the epidermis part of wheat straw are 150–200 nm in length and 20 nm in diameter.

Fig. 5 shows the typical SAXS two-dimensional scattering pattern of the wheat straw internodes, where the double-arrow indicated the longitude of the wheat straw stem. An equatorial streak scattering pattern, which usually do not contain maxima (as shown in the inset curves in Fig. 5), is obtained and it is indicated that cellulose crystals are in microfibrillar form. However, no equatorial streak will occur in the scattering pattern of a sample containing microfibrils if all microfibrils have the same average electron density, and furthermore are space filling (Balta-Calleja & Wonk, 1989). Therefore, it can be concluded that the cellulose microfibrils are not uniform in electron density, and the long period are broadened in the direction of the equator. The SAXS result mentioned above is similar to those of Jute, flax and ramie (Astley & Donald, 2001; Muller et al., 1998), but is different from those of wood that have a cross-like pattern corresponding to a helix-arrangement along the growth (Heyn, 1948, 1949, 1950).

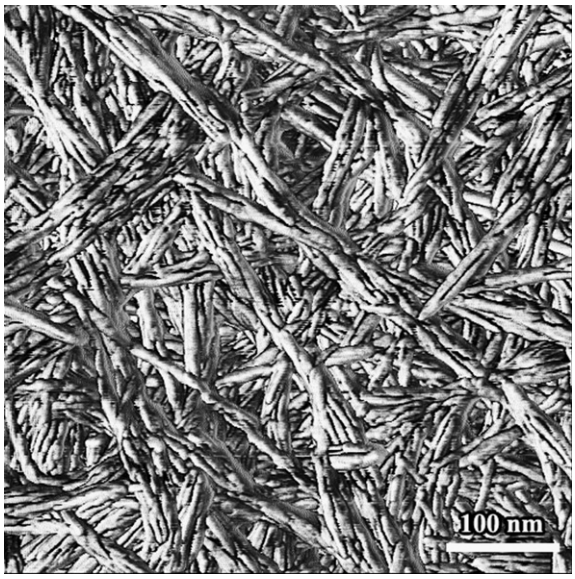

Fig. 4. AFM phase image of cellulose microcrystal produced by acidic hydrolysis.

The earlier work (Yu et al., 2005) has indicated that the annular ring exhibits negative optical property under the POM and the lamellae of cellulose in the annular ring are perpendicular to the tangential direction of the ring and arranged in sequence to form crystalline lamellae bundles that are around the annular. While in the spiral structure of cellulose crystal lamellar arranged by incline clockwise with an angle of about 30–40° to the tangential direction in the spiral vessel. The morphology and optical properties of the epidermal fiber are different from those of the annular ring and spiral structure of the vascular bundles, which means that the arrangement of the microfibrils and cellulose chains differs with those in annular ring and spiral structure of the vascular bundles. The arrangement of cellulose microfibrils and cellulose chains in the epidermal fiber of wheat straw is schematically shown in Fig. 6. The cellulose crystals in microfibrillar form, which are 20 nm in diameter and 150–200 nm in length, arrange periodically and longitudinally along the fiber axis. These fibrillar crystals are connected by amorphous regions of cellulose with a period of around 150–200 nm. The schematic mode of the

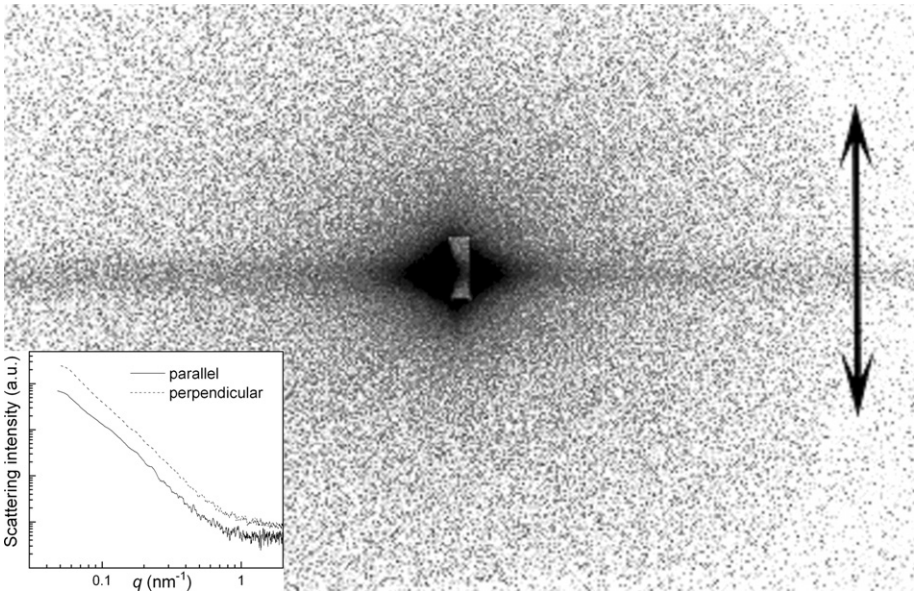

Fig. 5. SAXS pattern of the straw internodes. The arrow indicates the longitudinal direction. The inset figure shows the SAXS curves parallel and perpendicular direction to the longitude of the wheat straw.

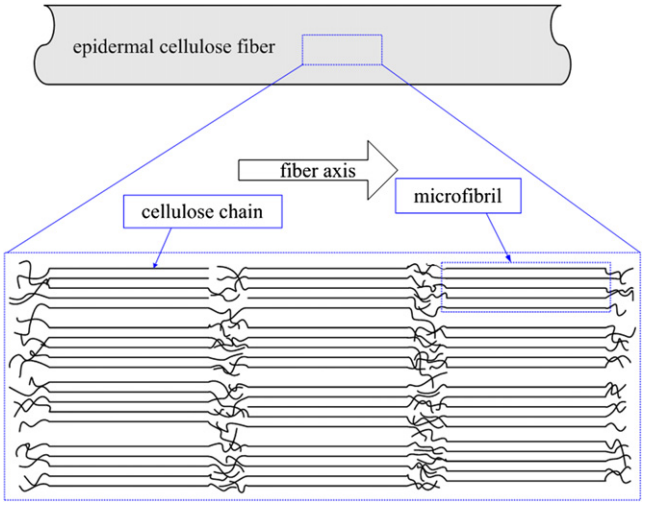

Fig. 6. Scheme of the arrangement cellulose microfibrils and cellulose chains in the epidermal fiber.

arrangement of cellulose fibrils and cellulose chains in the epidermal fiber of wheat straw is consistent with the theoretical model of the crystallized polymer proposed by Flory (Flory, Yoon, & Dill, 1984; Yoon & Flory, 1984). It is assumed, from this phenomenon, that microfibrils growing in the cell wall have to push their way through the existing components, leading to a number of structure defects, which may arise from dislocations at the interface of microcrystalline domains along the microfibrils length (Kuga & Brown, 1987; Revol, 1985).

4. Conclusion

Cellulose microfibrillar crystals arrange randomly in the parenchyma cell walls but arrange quite well longitudinal to the fiber axis in the epidermal fibers. The microfibrillar crystals are about 20 nm in diameter and 150–200 nm in length. Moreover, the cellulose microfibrillar crystals in the epidermal fibers align periodically along the fiber axis and the periodicity is similar to the length of the fibrillar crystals. This structure was confirmed by small angle X-ray scattering (SAXS).

Acknowledgements

The financial support by the National Natural Science Foundation of China (Grant No. 20374055, 50521302) and Chinese Academy of Sciences (Grant No. KJCX2-SW-H07) is greatly appreciated.

References

Astley, O. M., & Donald, A. M. (2001). A small-angle X-ray scattering study of the effect of hydration on the microstructure of flax fibers. *Biomacromolecules, 2*, 672–680.

Baker, A. A., Helbert, W., Sugiyama, J., & Miles, M. J. (1998). Surface structure of native cellulose microcrystals by AFM. *Applied Physics A-Materials Science & Processing, 66*, S559–S563.

Balta-Calleja, F. J., & Wonk, C. G. (1989). X-ray scattering of synthetic polymers. Amsterdam: Elsevier.

Campbell, N. A. (1993). Biology. Redwood City, CA: Benjamnin/Cumming Publishing Co. Inc.

Carpita, N. C., & Gibeaut, D. M. (1993). Structural models of primary-cell walls in flowering plants – Consistency of molecular-structure with the physical-properties of the walls during growth. *Plant Journal, 3*, 1–30.

Chanzy, H., & Henrissat, B. (1985). Undirectional degradation of valonia cellulose microcrystals subjected to cellulase action. *FEBS Letters, 184*, 285–288.

Davies, L. M., & Harris, P. J. (2003). Atomic force microscopy of microfibrils in primary cell walls. *Planta, 217*, 283–289.

Demirbas, A. (2004). Ethanol from cellulosic biomass resources. *International Journal of Green Energy, 1*, 79–87.

Dufresne, A., Kellerhals, M. B., & Witholt, B. (1999). Transcrystallization in Mcl-PHAs/cellulose whiskers composites. *Macromolecules, 32*, 7396–7401.

Flory, P. J., Yoon, D. Y., & Dill, K. A. (1984). The interphase in lamellar semicrystalline polymers. *Macromolecules, 17*, 862–868.

Gousse, C., Chanzy, H., Cerrada, M. L., & Fleury, E. (2004). Surface silylation of cellulose microfibrils: Preparation and rheological properties. *Polymer, 45*, 1569–1575.

Gunning, A. P., Cairns, P., Kirby, A. R., Round, A. N., Bixler, H. J., & Morris, V. J. (1998). Characterising semi-refined iota-carrageenan networks by atomic force microscopy. *Carbohydrate Polymers, 36*, 67–72.

Gustafsson, J., Ciovica, L., & Peltonen, J. (2003). The ultrastructure of spruce kraft pulps studied by atomic force microscopy (AFM) and X-ray photoelectron spectroscopy (XPS). *Polymer, 44*, 661–670.

Hanley, S. J., Giasson, J., Revol, J. F., & Gray, D. G. (1992). Atomic force microscopy of cellulose microfibrils – Comparison with transmission electron-microscopy. *Polymer, 33*, 4639–4642.

Hanley, S. J., Revol, J. F., Godbout, L., & Gray, D. G. (1997). Atomic force microscopy and transmission electron microscopy of cellulose from *Micrasterias denticulata*; evidence for a chiral helical microfibril twist. *Cellulose, 4*, 209–220.

Helbert, W., Cavaille, J. Y., & Dufresne, A. (1996). Thermoplastic nanocomposites filled with wheat straw cellulose whiskers. 1. Processing and mechanical behavior. *Polymer Composites, 17*, 604–611.

Heyn, A. N. J. (1948). Small angle X-ray scattering of various cellulose fibers. *Journal of the American Chemical Society, 70*, 3138–3139.

Heyn, A. N. J. (1949). Small-angle scattering of X-rays and the micellar structure in cellulose fibers. *Journal of the American Chemical Society, 71*, 1873–1875.

Heyn, A. N. J. (1950). Small angle X-ray scattering by cellulose fibers: Experimental study of the orientation factor in model filaments and rayons. *Journal of the American Chemical Society, 72*, 2284–2285.

Hornsby, P. R., Hinrichsen, E., & Tarverdi, K. (1997). Preparation and properties of polypropylene composites reinforced with wheat and flax straw fibres. 1. Fibre characterization. *Journal of Materials Science, 32*, 443–449.

Kim, N. H., Imai, T., Wada, M., & Sugiyama, J. (2006). Molecular directionality in cellulose polymorphs. *Biomacromolecules, 7*, 274–280.

Kondoh, K., Oginuma, H., Umeda, J., & Umeda, T. (2005). Innovative reuse of agricultural wastes as industrial raw materials to form magnesium composites. *Materials Transactions, 46*, 2586–2591.

Koyama, M., Helbert, W., Imai, T., Sugiyama, J., & Henrissat, B. (1997). Parallel-up structure evidences the molecular directionality during biosynthesis of bacterial cellulose. *Proceedings of the National Academy of Sciences of the United States of America, 94*, 9091–9095.

Kuga, S., & Brown, R. M. Jr., (1987). Practical aspects of lattice imaging of cellulose. *Journal of Electron Microscopy Technology, 6*, 349–356.

Liu, R. G., Yu, H., & Huang, Y. (2005). Structure and morphology of cellulose in wheat straw. *Cellulose, 12*, 25–34.

Liu, W. J., Mohanty, A. K., Askeland, P., Drzal, L. T., & Misra, M. (2004). Influence of fiber surface treatment on properties of Indian grass fiber reinforced soy protein based biocomposites. *Polymer, 45*, 7589–7596.

Maximova, N., Osterberg, M., Koljonen, K., & Stenius, P. (2001). Lignin adsorption on cellulose fibre surfaces: Effect on surface chemistry, surface morphology and paper strength. *Cellulose, 8*, 113–125.

Muller, M., Czihak, C., Vogl, G., Fratzl, P., Schober, H., & Riekel, C. (1998). Direct observation of microfibril arrangement in a single native cellulose fiber by microbeam small-angle X-ray scattering. *Macromolecules, 31*, 3953–3957.

Pesacreta, T. C., Carlson, L. C., & Triplett, B. A. (1997). Atomic force microscopy of cotton fiber cell wall surfaces in air and water: Quantitative and qualitative aspects. *Planta, 202*, 435–442.

Puglia, D., Tomassucci, A., & Kenny, J. M. (2003). Processing, properties and stability of biodegradable composites based on Mater-Bi-(R) and cellulose fibres. *Polymers for Advanced Technologies, 14*, 749–756.

Revol, J. F. (1985). Change of the d spacing in cellulose crystals during lattice imaging. *Journal of Materials Science Letters, 4*, 1347–1349.

Samir, M. A. S. A., Alloin, F., Sanchez, J. Y., & Dufresne, A. (2004). Cellulose nanocrystals reinforced poly(oxyethylene). *Polymer, 45*, 4149–4157.

Simola, J., Malkavaara, P., Alen, R., & Peltonen, J. (2000). Scanning probe microscopy of pine and birch kraft pulp fibres. *Polymer, 41*, 2121–2126.

Taiz, L., & Zeiger, E. (1991). *Cell walls: Structure, biogenesis and expansion. Plant Physiology*. Redwood City, CA: Benjamnin/Cumming Publishing Co. Inc.

Thimm, J. C., Burritt, D. J., Ducker, W. A., & Melton, L. D. (2000). Celery (*Apium graveolens* L) parenchyma cell walls examined by atomic force microscopy: effect of dehydration on cellulose microfibrils. *Planta, 212*, 25–32.

Yan, L. F., Li, W., Yang, J. L., & Zhu, Q. S. (2004). Direct visualization of straw cell walls by AFM. *Macromolecular Bioscience, 4*, 112–118.

Yoon, D. Y., & Flory, P. J. (1984). Chain Packing at Polymer Interfaces. *Macromolecules, 17*, 868–871.

Yu, H., Liu, R. G., Shen, D. W., Jiang, Y., & Huang, Y. (2005). Study on morphology and orientation of cellulose in the vascular bundle of wheat straw. *Polymer, 46*, 5689–5694.